Met. Mater. Int., Vol. 21, No. 5 (2015), pp. 923~928
doi: 10.1007/s12540-015-5050-1

Ti-Based Solid Solution Carbonitrides Prepared From Ti-Alloy Scraps via a Hydrogenation-Dehydrogenation Process and High-Energy Milling

Sun-A Jung, Hanjung Kwon*, Ki-Min Roh, Chang-Yul Suh, and Wonbaek Kim

Mineral Resources Research Division, Korea Institute of Geoscience and Mineral Resources, Yuseong-gu, Daejeon 305-350, Korea

(received date: 21 January 2015 / accepted date: 8 April 2015)

Ti-based solid-solution carbonitrides (Ti,Al,V)(CN) and (Ti,Al,Mo,V)(CN), were synthesized successfully using Ti-6Al-4V (Ti-64) and Ti-8Al-1Mo-1V (Ti-811) alloy scraps via hydrogenation-dehydrogenation and high-energy milling processes. A single phase of (Ti,Al,V)(CN) could be readily synthesized by the high-energy milling of Ti-64 alloy with graphite in a nitrogen atmosphere regardless of the carbon content. On the other hand, for the Ti-811 alloy, metallic Mo and various Mo-less carbides, in this case Ti_2AlC, Ti_3AlC_2, and Ti_3AlC, were also formed in addition to (Ti,Al,Mo,V)(CN) due to the low nitrogen affinity of Mo. The solid-solution carbonitrides consolidated by spark plasma sintering revealed excellent mechanical properties (H_V: 19.1-20.6 GPa, K_{IC}: 5.2-6.4 MPa·$m^{1/2}$) due to the alloying effect of Al, Mo, and V in Ti(CN). These values are superior to those of typical Ti(CN)–based ceramic composites (H_V: 16-20 GPa, K_{IC}: 3.2-5.5 MPa·$m^{1/2}$). We believe that the suggested method would be a valuable option for the production of Ti-based solid-solution carbonitrides with decent mechanical properties economically.

Keywords: ceramics, mechanical alloying/milling, toughness, indentation, nitridation

1. INTRODUCTION

Ti(CN) has been widely used in the manufacturing of cutting tools due to its good chemical stability and mechanical properties, i.e., high hardness and wear resistance [1-3]. Various additional carbides are usually added to improve the mechanical properties of Ti(CN) [1,4-9]. These include Mo_2C, VC, NbC, Cr_3C_2, TaC, and WC. Among them, Mo_2C is added to improve the sinterability by enhancing the wettability between the carbide and the matrix Ni when Ti(CN) is used as a cermet [1,4]. VC refines the microstructure by suppressing the grain growth of the hard phase by forming a solid solution because the crystal structure of VC is B1 (NaCl-like structure), which is identical to Ti(CN) [9]. Additionally, Al is known to improve the degree of high-temperature wear resistance by forming an Al_2O_3 layer [10-12].

Despite the improved properties of Ti(CN) with the addition of supplementary carbides, its relatively short lifetime hinders the wider application of Ti(CN) as a cutting tool material. More specifically, the relatively low toughness values of Ti(CN) compared to those of WC limits its application as a cutting tool material to specific milling operations. At present, Ti(CN) cutting tools are typically used for high-speed milling, semi-finishing, and finishing work for both carbon and stainless steels [13]. Recently, a solid-solution carbonitride (e.g., (Ti,M)(CN) (M=W, Mo, or V) was proposed as one means of resolving the issue of the low toughness of Ti(CN). Their fracture toughness was reportedly better than those of single-carbonitride materials [4,6,14,15].

The synthesis and mechanical properties of Ti-based solid-solution carbonitrides containing supplementary carbides of Al, V, and Mo have not been reported thus far. These can purportedly be prepared using a mixture of component carbides. However, such a process may not be feasible economically and may require excessive care so as to prevent undesirable interactions between each carbonitride phase. In view of this, we attempted to synthesize (Ti,Al,V)(CN), (Ti,Al,Mo,V)(CN) solid-solution carbonitrides using the most abundant Ti-based alloy scraps, i.e., Ti-6Al-4V (Ti-64) and Ti-8Al-1Mo-1V (Ti-811) [16,17]. Ti-64, Ti-811 alloy powders were prepared by the hydrogenation and dehydrogenation (HDH) process. The carbonitriding process was carried out by the high-energy milling of dehydrogenated alloy powders with carbon in an N_2 atmosphere. The carbonitriding behaviors of the Ti-64 and Ti-811 alloys were investigated in terms of the phase evolution during the milling and nitrogen affinity of the constituent elements in the alloys. The spark plasma sintering method was utilized to evaluate the mechanical properties of the product powders and the results were compared with

*Corresponding author: hanjungkwon@kigam.re.kr

those of previously reported Ti(CN)-based composites.

2. EXPERIMENTAL PROCEDURE

2.1. Hydrogenation-dehydrogenation (HDH) process with alloy scraps

The chemical compositions of the Ti-6Al-4V and Ti-8Al-1Mo-1V alloy scraps were measured by an ICP-AES (inductively coupled plasma-atomic emission spectrometer), with the result being 6.6 wt% Al, 4.2 wt% V (Ti-6Al-4V) and 7.9 wt% Al, 0.97 wt% Mo, 0.94 wt% V (Ti-8Al-1Mo-1V), respectively. The alloy scraps were cut into a proper size (10 mm × 10 mm × 10 mm) for the HDH process. The surface of each scrap was cleaned with acetone and alcohol. The Ti-64 and Ti-911 alloy scraps were then cleaned with acid cleaning solutions of $HCl:H_2O$ = 1:10 and $HF:H_2O$ = 1:10, respectively. After the surface cleaning process, they were dried for approximately 1 h under a vacuum atmosphere at a temperature of 473 K. For the purpose of pulverization by the HDH process, 100 g of the alloy was then inserted into a hydrogenation furnace. After a vacuum level of 1.3 Pa was reached, the furnace was heated to 873 K at 10 K/min and maintained at this level for 2 h. Afterwards, ultrapure hydrogen (99.9999%) was introduced into the furnace within a pressure range of 5×10^5-7×10^5 Pa. The hydrogenated alloy was crushed by hand with a hammer into evenly sized particles, after which the powders underwent a heat treatment for dehydrogenation in a vacuum of 6.7×10^{-3} Pa at 973 K for 2 h. A more detailed description of the HDH process is described in the literature [18].

2.2. High-energy milling of the alloy powders with carbon in an N_2 atmosphere

The dehydrogenated alloy powders were then mixed with graphite at ratios of 1:0.3, 1:0.5, 1:0.7 and 1:1 (the molar ratio of the metal elements and carbon). The powders were subjected to high-energy ball milling using a planetary mill (Model Pulverisette 5, Fritsch, Germany). Tungsten carbide balls were mixed with the alloy powders at a ball-to-powder weight ratio of 40:1. A stainless steel bowl was used, and all milling processes were conducted at a speed of 250 RPM for 20 hr in a nitrogen atmosphere of 1 atm. The synthesized (Ti,Al,V)(CN) and (Ti,Al,Mo,V)(CN) powders were annealed at 1200 °C for 2 h in a graphite furnace under a vacuum to eliminate the oxygen induced by the milling processes. The phase evolutions during the milling process were analyzed using an X-ray diffractometer (Smartlab, Rigaku, Japan) with monochromatized Cu-Kα radiation (λ=1.5418 Å) and Si (SRM640D, NIST, USA) as a standard. Nonmetallic elements such as carbon, nitrogen and oxygen were analyzed with a Leco C/N/O analyzer. A field-emission scanning electron microscopy (FE-SEM) attachment (Quanta 650, FEI, Oregon, USA) was used to analyze the morphologies of the synthesized powders.

2.3. Spark plasma sintering of synthesized (Ti,Al,V)(CN) and (Ti,Al,Mo,V)(CN) powders

The synthesized powders were placed in a graphite die (outside diameter, 35 mm; inside diameter, 10 mm; height, 40 mm) and were introduced into the SPS system (Eltek, South Korea). The sintering process was conducted typically in four stages. The system was evacuated (stage 1) and subjected to a uniaxial pressure of 80 MPa (stage 2). An induced current was activated and maintained until densification occurred, as indicated by a linear gauge which measured the degree of sample shrinkage (stage 3). The temperature was measured by an optical pyrometer that was focused on the surface of the graphite die. Sintering continued until the shrinkage reached a constant value at 1700 °C. Afterwards, the compact was cooled to room temperature (stage 4). The Vickers hardness levels of the sintered (Ti,Al,V)(CN) and (Ti,Al,Mo,V)(CN) bodies were measured with an indenter load of 20 kg, and the fracture toughness was calculated using the expression derived by Shetty *et al*. [19].

3. RESULTS AND DISCUSSION

3.1. HDH of Ti-64 and Ti-811 alloys

Figure 1 shows the X-ray diffraction patterns of the alloys during the HDH process. Here, (b) and (c) correspond to the patterns of the Ti-64 and Ti-811 alloys after hydrogenation, respectively, whereas (d) and (e) correspond to the patterns of the Ti-64 and Ti-811 alloys after dehydrogenation. The hydrogenation treatment did not produce a single-hydride phase for both alloys. The alloy was transformed mostly to the TiH_2-type hydride phase (■) with a small amount of α-Ti (●) remaining. The lattice parameter of the phase was smaller than that of pure α-Ti. We presume that it is α-(Ti,Al) or α-

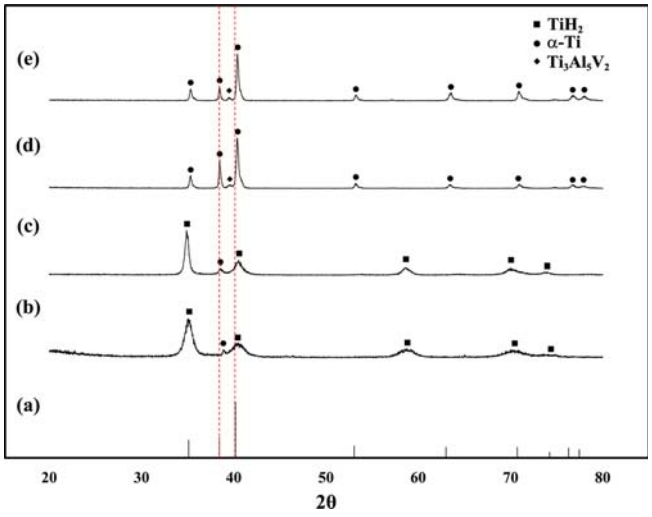

Fig. 1. X-ray diffraction patterns of (a) JCPDS card (α-Ti, entry #: 441294), (b) hydrogenated Ti-64 alloy, (c) hydrogenated Ti-811 alloy, (d) dehydrogenated Ti-64 alloy, and (e) dehydrogenated Ti-811 alloy.

(Ti,Al,V), as the atomic radii of Al and V are smaller than that of Ti. The standard Gibbs free energy of formation for AlH_3 is 46.875 kJ/mole at 300 K and 66.701 kJ/mole at 400 K (positive values) [20]. Therefore, it is feasible that Al does not participate in the hydride-forming reaction during the HDH process, dissolving into α-Ti instead.

The dehydrogenation of the hydrogenated Ti-64 and Ti-811 alloys was carried at 973 K for 2 h in a vacuum. This process transformed the alloy hydride phase into the α-Ti phase, with a small amount of the $Ti_3Al_5V_2$ intermetallic phase. They were mixed with carbon at a specified ratio and high-energy milled under 1 atm of N_2.

3.2. High-energy milling of Ti-64 and Ti-811 alloys

Figure 2 shows the X-ray diffraction patterns of the dehydrogenated Ti-6Al-4V alloy after milling with graphite in 1 atm of N_2. Here, the carbon/metal ratios were 0.5(a), 0.7(b), and 1(c). Figure 2 clearly shows that a single-phase carbonitride was synthesized regardless of the initial carbon content. However, it should be noted that there is the peak shift towards a higher angle with a decrease in the initial carbon content. This suggests that the lattice parameter of the carbonitride decreases as the carbon content is decreased. This may be possible with the simple reduction of the carbon content in the lattice and/or by the substitutional incorporation of nitrogen into the lattice, which has a smaller atomic size than carbon. On the other hand, the high-energy milling of the dehydrogenated Ti-811 alloy produced a number of phases depending on the amount of carbon added (Fig. 3). Here, the carbon/metal ratios were 0.3(a), 0.5(b), 0.7(c), and 1(d) with the N_2 pressure fixed at 1 atm. At the ratios of 1 and 0.7, a single-phase carbonitride (■) was synthesized ((c) and (d)). When the ratio was lowered to 0.5, Ti_2AlC (●) and Ti_3AlC_2 (▲) phases were formed in addition to the carbonitride phase (See (d)). When the ratio was decreased further

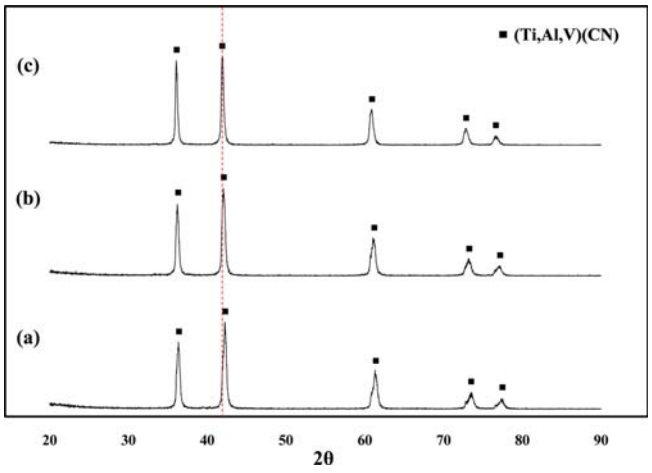

Fig. 2. X-ray diffraction patterns of Ti-64 + C after milling at different carbon/metal ratios: (a) 0.5 (b) 0.7, and (c) 1.

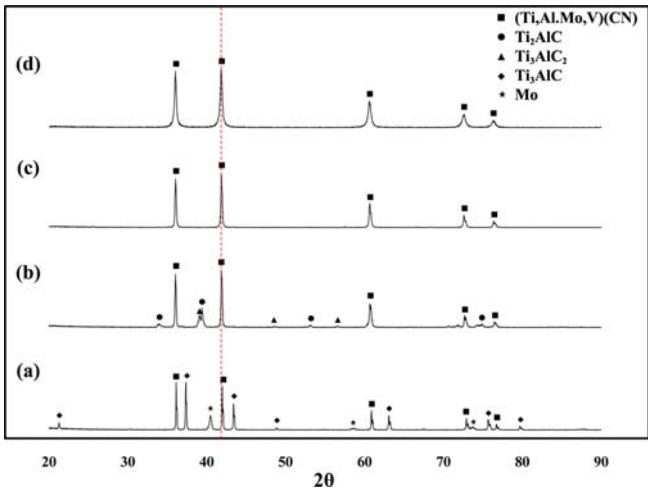

Fig. 3. X-ray diffraction patterns of Ti-811 + C after milling at different carbon/metal ratios: (a) 0.3 (b) 0.5, (c) 0.7, and (d) 1.

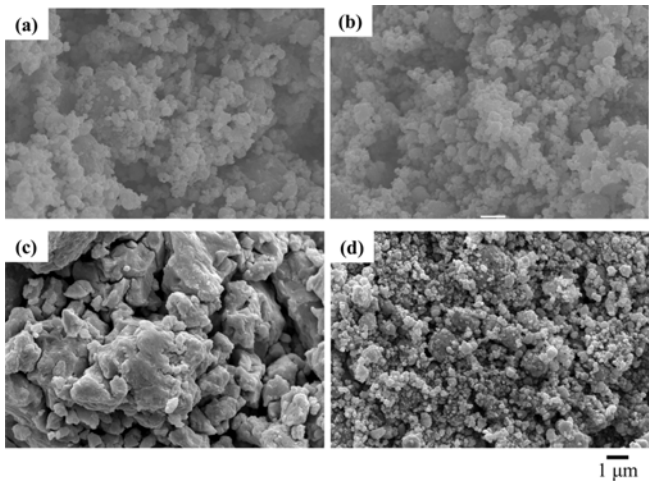

Fig. 4. Powder morphologies of the milled powders of (a) Ti-64 + C at a carbon/metal ratio of 0.3, (b) Ti-64 + C at a carbon/metal ratio of 1, (c) Ti-811 + C at a carbon/metal ratio of 0.3, and (d) Ti-811 + C at a carbon/metal ratio of 1.

to 0.3, the metallic Mo and Ti_3AlC (◆) phases appeared.

The difference in the phase evolution during the high-energy milling of Ti-64 and Ti-811 alloys could also be recognized in FE-SEM images. Fig. 4 shows the dehydrogenated Ti-64 and Ti-811 alloys after milling. Here, (a) and (b) are images of the Ti-64 alloys and (c) and (d) are images of the Ti-811 alloys for carbon/metal ratios of 0.3 and 1.0, respectively. For the Ti-64 alloy, the powder morphology was similar in both cases (See Figs. 4(a) and (b)). This is feasible, as the high-energy milling of Ti-64 produced only a single-phase carbonitride regardless of the carbon content. However, for the Ti-811 alloy, the powder morphology is significantly different; large and heavily agglomerated (see Fig. 4(c)). As mentioned previously, the milled powder of Ti-811 with the carbon/metal ratio of 0.3 contained the metallic Mo and Ti_3AlC phases.

Table 1. Carbon and nitrogen content in Ti-811 and Ti-6Al-4V carbonitride samples[a]

Raw material	Carbon/metal molar ratio of raw material	Carbon (wt%)	Nitrogen (wt%)	Chemical formula
Ti–64	0.5	8.49 (0.1)	12.35 (0.05)	$(Ti_{0.86}Al_{0.10}V_{0.04})(C_{0.45}N_{0.55})$
	0.7	11.3 (0.1)	9.76 (0.01)	$(Ti_{0.86}Al_{0.10}V_{0.04})(C_{0.57}N_{0.43})$
	1	16.6 (0.1)	6.26 (0.07)	$(Ti_{0.86}Al_{0.10}V_{0.04})(C_{0.76}N_{0.24})$
Ti–811	0.3	7.1 (0.2)	1.30 (0.00)	-
	0.5	10.9 (0.2)	1.51 (0.02)	-
	0.7	15.4 (0.1)	1.73 (0.01)	$(Ti_{0.83}Al_{0.15}Mo_{0.01}V_{0.01})(C_{0.93}N_{0.07})$
	1	19.5 (0.2)	1.21 (0.02)	$(Ti_{0.83}Al_{0.15}Mo_{0.01}V_{0.01})(C_{0.95}N_{0.05})$

[a]Standard deviation in parentheses

Thus, it was considered that the metallic phase, which is ductile, made the powder particles agglomerate and become larger.

The result described above clearly demonstrates that the synthesis of single-phase (Ti,Al,Mo,V)(CN) is not easy, especially for conditions with lower carbon contents. Table 1 lists the carbon and nitrogen measurements of the milled powders of the Ti-64 and Ti-811 alloys. The chemical formulae of the single-phase (Ti,Al,V)(CN) and (Ti,Al,Mo,V)(CN) are also shown. It is clear that the nitrogen contents in the milled powders of the Ti-64 alloy are significantly higher than those in the milled powders of the Ti-811 alloy. Figure 5 clearly explains the different carbonitriding behaviors of the two alloys. For the Ti-64 alloy, the carbon content of the milled powders increases linearly due to the increase in the input carbon content. In the meantime, nitrogen is shown to decrease sharply, suggesting that the content of nitrogen incorporated into the lattice is reduced. In comparison, the carbonitriding behavior of the Ti-811 alloy is significantly different. The carbon content in the Ti-811 alloy behaves similarly depending on initial carbon content. Nevertheless, the amount of nitrogen is nearly constant regardless of the carbon content. The comparison of the two alloys suggests that the nitriding characteristics of both alloys are significantly different despite

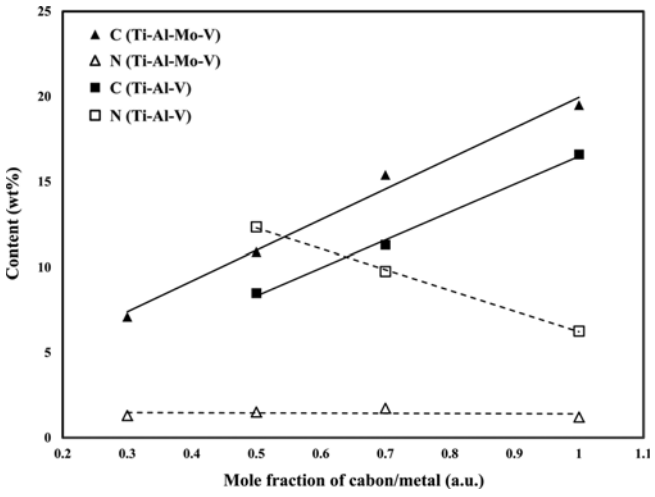

Fig. 5. The effect of carbon/metal ratio on the carbon and nitrogen contents in the milled powders of Ti-64 + C and Ti-811 + C.

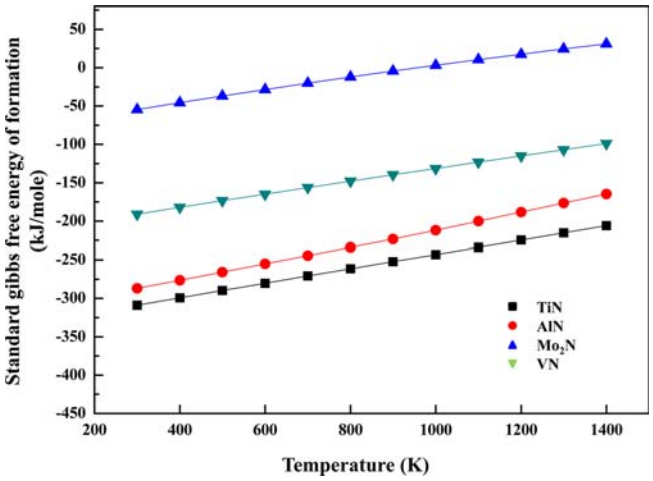

Fig. 6. Standard Gibbs free energy of formation values of the Ti, Al, Mo, and V nitrides [20].

their similar alloy compositions. Here, the main difference between the two alloys is the presence of Mo. Naturally, the answer may be found in the nitridation behavior of Mo.

3.3. Nitridation of the Ti-811 alloy

The nitridation energy of the constituent elements in Ti-811 alloy was examined while considering the free energy of their nitrides. Figure 6 shows the standard Gibbs free energy of formation of their nitrides. It was noted that TiN, AlN and VN have negative free energy and that they are stable up to 1400 K. In contrast, Mo_2N is unstable when the temperature exceeds approximately 1000 K. The equilibrium nitrogen partial pressures for nitride formation are as follows:

$$Ti_{(s)} + 1/2N_{2(g)} \rightarrow TiN_{(s)},\ p_{N_2} = 4.4 \times 10^{-16}\text{atm} \quad (1)$$

$$Al_{(s)} + 1/2N_{2(g)} \rightarrow AlN_{(s)},\ p_{N_2} = 5.0 \times 10^{-13}\text{atm} \quad (2)$$

$$2Mo_{(s)} + 1/2N_{2(g)} \rightarrow Mo_2N_{(s)},\ p_{N_2} = 210.6\ \text{atm} \quad (3)$$

$$V_{(s)} + 1/2N_{2(g)} \rightarrow VN,\ p_{N_2} = 4.1 \times 10^{-8}\text{atm} \quad (4)$$

This simple calculation demonstrates that Mo requires 210

Table 2. Mechanical properties of of the sintered carbonitrides along with those of other structural ceramics.[a]

Materials	H_V (GPa)	K_{IC} (MPa·m$^{1/2}$)
$(Ti_{0.86}Al_{0.10}V_{0.04})(C_{0.45}N_{0.55})$	19.8 (0.4)	6.0 (0.3)
$(Ti_{0.86}Al_{0.10}V_{0.04})(C_{0.57}N_{0.43})$	20.6 (0.1)	6.2 (0.6)
$(Ti_{0.86}Al_{0.10}V_{0.04})(C_{0.76}N_{0.24})$	19.2 (0.1)	6.4 (0.5)
$(Ti_{0.83}Al_{0.15}Mo_{0.01}V_{0.01})(C_{0.95}N_{0.05})$	19.1 (0.3)	5.2 (0.2)
Ti(CN)-based composites [21]	16 – 18	3.5 – 5.5
Commercial Al_2O_3-TiC composite	20	3.2

[a]Standard deviation in parentheses

atm to from a nitride, which is much higher than the value of 1 atm in this study [21]. It is clear that Mo is the critical element in the carbonitriding reaction of the Ti-811 alloy.

3.4. Mechanical properties of sintered (Ti,Al,V)(CN) and (Ti,Al,Mo,V)(CN)

The mechanical properties of (Ti,Al,V)(CN) and (Ti,Al, Mo,V)(CN) consolidated by SPS are summarized in Table 2, along with the corresponding data for commercial structural ceramics and their composites. The hardness values of the sintered carbonitrides from the alloy scraps were nearly identical regardless of the composition. These values were in the range of 19.1-20.6 GPa for the sintered carbonitrides, higher than those of Ti(CN)-based compositess (composites in the form of a simple mixture: Ti(CN)-Mo_2C, Ti(CN)-TaC, Ti(CN)-NbC, Ti(CN)-WC) (16-17 GPa) and also equivalent to those of the commercial Al_2O_3-TiC composite (hardness of 20 GPa; Product BX20, Korloy Co., Ltd.), which is currently used as a commercial cutting tool material [22]. Meanwhile, the fracture toughness levels of (Ti,Al,V)(CN) and (Ti,Al,Mo,V) (CN) from the alloy scraps ranged from 5.2 to 6.4 MPa·m$^{1/2}$. These values are significantly better than those of both a previously reported Ti(CN)-based composites (K_{IC}: 3.5-5.5 MPa·m$^{1/2}$) and the commercial Al_2O_3-TiC composite (K_{IC}: 3.2 MPa·m$^{1/2}$). The improved toughness can be attributed to the alloying effects of Al, Mo, and V in the Ti(CN), as discussed in previous studies [4,6,14,15].

4. CONCLUSION

In this paper, Ti-based solid-solution carbonitrides, (Ti,Al,V) (CN) and (Ti,Al,Mo,V)(CN), were successfully fabricated using Ti-6Al-4V (Ti-64) and Ti-8Al-1Mo-1V (Ti-811) alloy scraps via hydrogenation-dehydrogenation (HDH) and high-energy milling processes. After the hydrogenation process, the α-(Ti,Al) or the (Ti,Al,V) phase remained due to the low stability of the AlH_3 phase ($\Delta G_f^{AlH_3}$ =66.701 kJ/mole at 400 K). When the dehydrogenated Ti-64 and Ti-811 alloy powders were reacted with carbon and nitrogen by high-energy milling, carbonitridation of the Ti-64 alloy was readily achieved, whereas that of the Ti-811 alloy occurred only partially due to the thermodynamic instability of the Mo nitride. The high Gibbs free energy of formation of Mo_2N ($\Delta G_f^{Mo_2N}$ = 31.143 kJ/mole at 1400 K) was the cause of the limited nitridation of the Ti-811 alloy as compared to that of the Ti-64 alloy. The spark-plasma-sintered (Ti,Al,V)(CN) and (Ti,Al,Mo,V) (CN) from the alloy scraps showed improved toughness levels (5.2-6.4 MPa·m$^{1/2}$) compared to those of previously reported Ti(CN)-based composites (K_{IC}: 3.5-5.5 MPa·m$^{1/2}$) and the commercial Al_2O_3-TiC composite (K_{IC}: 3.2 MPa·m$^{1/2}$). Based on these results, we suggest that the proposed method can be used to produce various Ti-based solid-solution carbonitrides with decent mechanical properties economically.

ACKNOWLEDGEMENT

This work was supported by a Grant-in-Aid from the Basic Research Project of the Korea Institute of Geoscience and Mineral Resources (KIGAM), funded by the Ministry of Science, ICT and Future Planning (GP2012-019).

REFERENCES

1. P. Ettmayer, *Annu. Rev. Mater. Sci.* **19**, 145 (1989).
2. S. Kang, *Comprehensive Hard Materials* (eds. D. Mari, L. Llanes, and C. E. Nebel), pp. 139-181, Elsevier Ltd., Boston (2014).
3. Y. Choi, *Met. Mater. Int*. **20**, 531 (2014).
4. J. Jung and S. Kang, *J. Am. Ceram. Soc.* **90**, 2178 (2007).
5. S. Kim, K.-H. Min, and S. Kang, *J. Am. Ceram. Soc.* **86**, 1761 (2003).
6. J. Jung and S. Kang, *Acta Mater.* **52**, 1379 (2004).
7. S. Zhou, W. Zhao, and W. Xiong, *Int. J. Refract. Met. Hard Mater.* **27**, 26 (2009).
8. W. Wan, J. Xiong, Z. Guo, H. Du, and L. Tang, *Int. J. Refract. Met. Hard Mater.* **45**, 86 (2014).
9. Y. Peng, H. Miao, and Z. Peng, *Int. J. Refract. Met. Hard Mater.* **39**, 78 (2013).
10. P. H. Mayrhofer, C. Mitterer, L. Hultman, and H. Clemens, *Prog. Mater. Sci.* **51**, 1032 (2006).
11. A. Horling, L. Hultman, M. Oden, J. Sjolen, and L. Karlsson, *Surf. Coat. Tech.* **191**, 384 (2005).
12. G. S. Fox-Rabinovich, J. L. Endrino, B. D. Beake, A. I. Kovalev, S. C. Veldhuis, L. Ning, F. Fontaine, and A. Gray, *Surf. Coat. Tech.* **201**, 3524 (2006).

13. E. B. Clark and B. Roebuck, *Int. J. Refract. Met. Hard Mater.* **11**, 23 (1992).
14. S. Park and S. Kang, *Scripta Mater.* **52**, 129 (2005).
15. J. Jung and S. Kang, *Script Mater.* **56**, 561 (2007).
16. G. Y. Yoo, C. H. Park, J.-K. Hong, S.-E. Kim, N. H. Kang, and J.-T. Yeom, *Korean J. Met. Mater.* **51**, 307 (2013).
17. T. Moskalewicz, S. Zimowski, B. Wendler, P. Nolbrzak, and A. Czyrska-Filemonowicz, *Met. Mater. Int.* **20**, 269 (2014).
18. J. M. Oh, K. M. Roh, B. K. Lee, C. Y. Suh, W. Kim, and H. Kwon, *J. Alloys Compd.* **593**, 61 (2014).
19. D. K. Shetty, I. G. Wright, P. N. Mincer, and A. H. Clauer, *J. Mater. Sci.* **20**, 1873 (1985).
20. I. Barin, *Thermochemical Data of Pure Substances*, pp.42-1628, VCH Verlagsgesellschaft mbH, Weinheim (1989).
21. H. Jehn and P. Ettmayer, *J. Less-common Met.* **58**, 85 (1978).
22. D. S. Park and Y. D. Lee, *J. Am. Ceram. Soc.* **82**, 3150 (1999).